

# Gradient Based Optimization of Permanent Magnet Generator Design for a Tidal Turbine

Astrid Røkke

Department of Electric Power Engineering  
Norwegian University of Science and Technology (NTNU)  
Trondheim, Norway  
Email: astrid.roekke@ntnu.no

**Abstract**—An optimization of an analytical problem with nine variables is executed to find the optimal Permanent Magnet (PM) generator for a tidal turbine. A gradient based solver is used to find the minimum cost of active materials for the given design specifications. The MATLAB function *fmincon* is used, and the possible minimization algorithms available for this function are compared. As these solvers are only able to find a local minimum, a search is performed trying to find other minimas, both using a *MultiStart* procedure and using a Genetic Algorithm (GA). Losses are calculated for windings, stator laminations and rotor magnets and solid steel, and a constraint is put on efficiency. The cost effect of varying this constraint is investigated. Optimizations are done with both weight and material cost as objective function, and the different resulting designs are presented.

## I. INTRODUCTION

### A. Problem formulation

The goal of this paper is to find the best possible electromagnetic design for a generator in a tidal turbine. The tidal industry is in a phase of development, and developers are struggling to find economically viable solutions, hence it is important that each component of the system is as cost-effective as possible. Based on a study of existing and developing tidal technology [1], a set of specifications and constraints have been chosen. The generator is designed for a central shaft turbine with a one-stage gear. A one-stage gear is a trade-off between cost and weight on one side, and reliability and efficiency on the other. The design specifications are listed in Table I. The generator will be a surface mounted PM machine with concentrated windings. The number of poles and slots are restricted to  $22 \cdot n_{base}$  and  $24 \cdot n_{base}$ , respectively, where  $n_{base}$  is the number of base windings. The chosen combination of poles and slots will result in a machine with low cogging torque and a simple assembly. Other slot pole combinations might prove to be more purposeful. This will be investigated later. Because of the winding layout, subharmonic fields are present, causing losses in the rotor magnets and rotor yoke, which is to be built with solid magnetic steel due to cost and

TABLE I  
DESIGN SPECIFICATIONS

Turbine power	1,5 MW
Mechanical speed	80 rpm
Air gap length	6 mm
Number of phases	3
Line to line voltage	3,3 kV

material savings. The generator will be air filled and cooled by the water flowing around it.

The objective function is an estimate of the price of active materials. The effect of choosing another objective function; weight, is also illustrated. Optimizations of electrical machines are often done for the rotor given a specific stator, or vice versa. Even better results can be achieved if both rotor and stator geometry are allowed to vary. As many as possible of the design parameters are chosen to be variables. If magnetic flux densities in different parts of the machine were set as input parameters, and dimensions set according to this, it would threaten the optimality of the solution, because the chosen flux density might not prove to be optimal at all.

Optimization variables are listed in Table II, and visualized in Figure 1.  $\alpha_m$  is defined as  $w_m/\tau_p$ , and  $h_{wind}$  and  $w_{wind}$  are winding height and width. Design details like pole shoes, slot wedges and magnet shape are left out of the scope. Constraints are set for different parameters listed in III based on typical requirements for the tidal power industry. These constraints are not necessarily final, but based on practicalities and expectations from the tidal power industry. The possible savings made by relaxing some of these constraints are investigated. The optimization is performed with the MATLAB optimization toolbox, using the built-in minimization function *fmincon*. This is a nonlinear solver that can solve unconstrained, linearly constrained and nonlinearly constrained problems. The optimization technique is deterministic and employs the gradient or the Hessian of the objective function to establish a search direction. Common for this type of method is that the found solution might be a local minimum, and not a global one. The selected starting point of the search will influence which minimum you end up with. A multistart procedure is

TABLE II  
OPTIMIZATION VARIABLES

Variables			lower	upper
$D_{outer}$	Outer diameter	m	0	3.5
$d_{s,yoke}$	Stator yoke thickness	mm	5	inf
$d_{slot}$	Slot depth	mm	6	inf
$w_{slot}$	Slot width	mm	4.4	inf
$l_m$	Magnet length	mm	2	100
$\alpha_m$	Magnet width/pole pitch		0.01	0.99
$d_{r,yoke}$	Rotor yoke thickness	mm	5	inf
$J$	Current density	A/mm <sup>2</sup>	0	4
$n_{base}$	Number of base windings		1	13

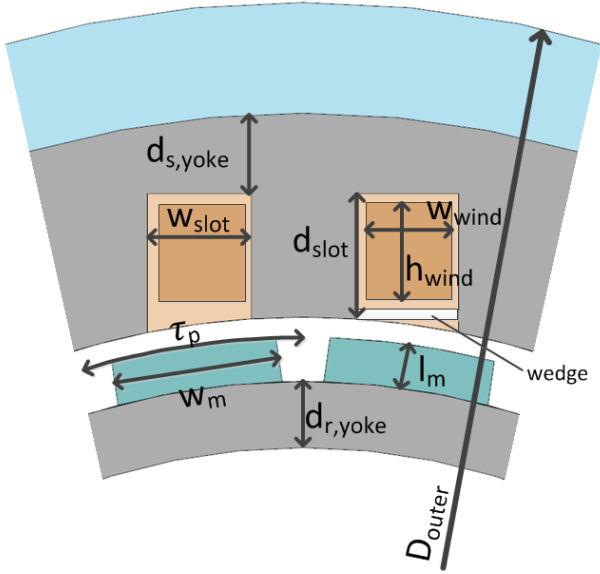


Fig. 1. Geometric variables. Parameter information is listed in Table II

performed to check for multiple minimas, and a GA is used to compare the results and verify that the result is, in fact, a global minimum. Gradient based solvers are unable to solve problems with integer number variables. This is a serious limitation when optimizing electrical machines, since the number of slots and poles must always be integer. The choice of interior vs. surface mounted PMs and the choice of rotor and stator yoke material are other parameters of interest that could be included as integer variables. In this work, an outer loop is created to optimize the number of base windings.

### B. Previous work

For many years, much focus has been put on optimization of electrical machines and on PM machines in particular [2]–[4]. [5] presents an overview of different optimization methods used for design of electrical machines. Optimization methods can mainly be categorized as either gradient based or direct optimization or a combination of both, although there are examples of other methods too. Direct optimization only needs the numerical value of the objective function, while gradient-based optimizations require a gradient to find a search direction and determine how far to move in that direction. The last is a fast and efficient way to find a local solution, but is unable to search for multiple minimas, and therefore risks finding a local, and not a global minimum. It also requires a smooth objective function, and cannot have integer number variables. Evolutionary Algorithms, including GAs, are examples of direct optimization techniques that are able to find the area of the global minimum. GA have been widely used in optimization of electrical machine design [3], [6], [7], however, other evolutionary algorithms, like Immune Algorithms, Evolution Strategy, Differential Evolution [8], [9] and Particle Swarm Optimization [10] also show good results. In many cases, a hybrid solution is employed, where an Evolutionary Algorithm is used to find the area of the global

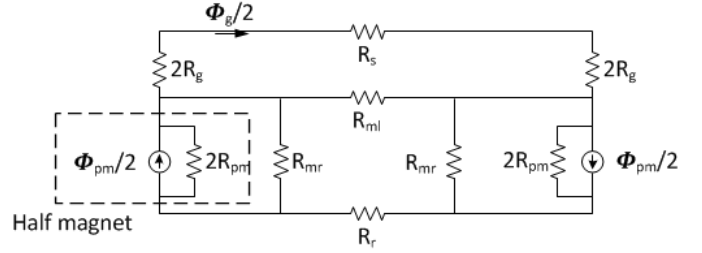


Fig. 2. No-load magnetic circuit

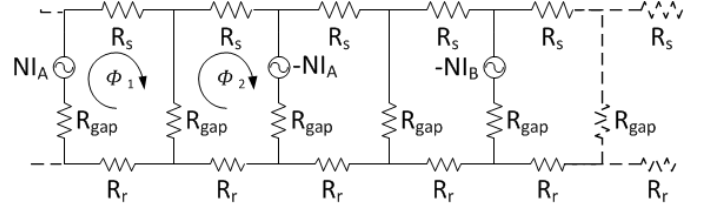


Fig. 3. Section of armature reaction circuit

minimum, and a local search algorithm is used to find the precise location of the minimum [4], [11], [12]. This reduces the number of evaluations drastically.

It has been argued that a global optimization technique is necessary for machine design optimization, because of the existence of many local minimas. Despite this, many authors have used different nonlinear programming algorithms in this area. In [13], [14] Sequential Quadratic Programming (SQP) methods are used to optimize synchronous reluctance motors. Published papers on optimization of electrical machines rarely provide advices on details regarding the optimization procedure, like setting bounds and choice of algorithm within deterministic nonlinear methods. This paper will show how the electrical machine design is optimized and also give some specific guidance to the reader.

## II. THE MACHINE MODEL

### A. The electromagnetic model

The electromagnetic model is based on a lumped parameter network shown in Figure 2 [15].  $R_s$  and  $R_r$  are stator and rotor yoke reluctance. Both are set to zero because of the high relative permeability of iron.  $R_g$  is the air gap reluctance,  $R_{ml}$  is the magnet to magnet leakage reluctance,  $R_{mr}$  is the magnet to rotor yoke leakage reluctance,  $R_{pm}$  is magnet reluctance and  $\phi_{pm}$  is remanent flux of the permanent magnet. The physical air gap is multiplied with a Carter coefficient to account for the variation of flux density in the air gap caused by slotting. No-load magnetic flux densities are estimated for torque prediction and for iron-loss prediction. In order to investigate the effect of the different harmonics produced by the stator on the rotor, the magnetic circuit shown in Figure 3 is used to find the electric loading and magneto-motive force in loaded condition.  $R_{gap}$  is the reluctance of the magnet and the air gap combined,  $N$  is the number of turns per coil,  $I_A$  and  $I_B$  are the currents of phase A and B, respectively and  $\phi_1$  and  $\phi_2$  are the mesh fluxes in the first and second loop.

The figure shows only 4-5 loops in a mesh network. With the given slot and pole combination the total number of loops is 24. For any number of  $n_{base}$ , the flux pattern is symmetrical about 24 slots. For the second loop, the mesh equation

$$(\phi_2 - \phi_1)R_{gap} + \phi_2 R_s - NI_A + (\phi_2 - \phi_3)R_{gap} + \phi_2 R_r = 0 \quad (1)$$

is true. The flux passing through the tooth between the two first loops is  $\phi_1 - \phi_2$ . The harmonic content of the electric loading is employed in the calculation of rotor loss.

Magnetic saturation is not included in the model. However, the magnetic flux density is constrained in stator teeth, stator back yoke and rotor back yoke, the values can be seen in Table III. The magnetic flux density is calculated for flux produced by magnets alone and flux produced by stator currents alone, and a constraint is put on each case. The two values should not be added, because the flux will have a phase shift of  $\pi/2$  when current is placed in the q-axis.

Produced torque is found with the following equation,

$$T = \frac{3}{2} p \phi_g \frac{Q}{6} k_w \hat{I}_s L \quad (2)$$

where  $p$  is the pole pair number,  $\phi_g$  is the air gap flux per pole at no-load,  $Q$  is the number of slots,  $k_w$  is the winding factor,  $\hat{I}_s$  is the amplitude of the slot current and  $L$  is the active length.

### B. The electric model

The slot is modelled as shown in 1 with a slot wedge at the slot opening. The winding is fitted with a slot insulation layer of constant thickness, and the fill factor of the coil inside this is set to a fixed value. The number of turns is automatically chosen to obtain a voltage rating of approximately 3.3 kV. Slot inductance, air gap inductance and end winding inductance are calculated according to [15], and resistance calculations include end winding resistance. For the sake of simplicity, it is assumed that the current is placed in the q-axis, ensuring maximum torque per ampere. Later work could include power factor angle as a variable, and cost of the converter can be included in the objective function.

### C. The mechanical model

Mechanical structures are not included in the model, with exception of the outer housing wall, the thickness of which is set to 5 cm regardless of diameter and length. The cost and weight of this are included in the objective functions. One mechanical constraint is included in the model, namely the maximum shear stress of the rotor shaft. The rotor yoke can, for small diameter machines, act as the shaft, and the shaft stress is to be kept below 30 MPa in a case where the outer diameter of the rotor yoke equals the shaft diameter.

$$T = \frac{J_T}{r} \tau \quad (3)$$

where  $T$  is torque,  $\tau$  is maximum shear stress,  $r$  is the radius and  $J_T = \pi r^4 / 2$  is the torsion constant for a circular cross-section.

### D. Losses

Losses are found for windings, stator laminations, rotor yoke and magnets.

Copper loss is found for both the active section and the end windings. As the exact dimensions of the winding wire is not known, the AC losses are not calculated, but estimated as 1.2 times the DC losses. Copper losses are calculated for a temperature of 90 °C. For further improvement of the model, copper temperatures can be calculated with a thermal model, and this temperature can be used to find real copper resistance. Iron losses are estimated with the equation below, combining hysteresis loss,  $p_h$  and eddy current loss,  $p_e$  with a given magnetic flux density  $B$  and angular frequency  $\omega$ :

$$p_{iron} = p_h + p_e = k_h B^\beta \omega + k_e B^2 \omega^2 \quad (4)$$

$k_h$ ,  $k_e$  and  $\beta$  are hysteresis and eddy current coefficients, with values found in [16]. The expression is valid for sinusoidal flux density. Only the no-load flux density is used in iron-loss calculations.

Magnet losses and eddy current losses induced in the solid rotor yoke are calculated by the method found in [17], [18]. This method efficiently takes all harmonics produced by the stator into account, which is of particular importance in machines with single layer concentrated windings, where especially the low order harmonics can cause large rotor losses.

Friction losses are not included in the model. It is assumed that these will be of approximately the same magnitude independent of the geometric dimensions. Consequently, the calculated efficiency will be slightly higher than the actual efficiency of the generator.

## III. OPTIMIZATION MODEL

### A. MATLAB optimization algorithms

Constrained minimization is the task of finding the set  $n$  of variables  $\mathbf{X}=(x_1, \dots, x_n)$  that result in the lowest possible scalar value  $f(\mathbf{X})$  subject to a set of  $m$  constraints,  $G_k(\mathbf{X}) \leq 0$ ,  $k=1, \dots, m$ . The feasible region is the set of  $\mathbf{X}$  where all constraints  $G_k(\mathbf{X}) \leq 0$  are satisfied.

The minimization function *fmincon* can employ four different algorithms; *Trust region reflective*, *interior point*, *active set* and *SQP* [19]. The *Trust region reflective* algorithm cannot be used for problems with nonlinear constraints. The *interior point* algorithm uses a *Barrier Function* to stay within the feasible region. For each iteration, either a Newton step, where the Karush Kuhn Tucker equations are solved via linear approximation, or a Conjugate gradient method, based on the steepest descent, is used to obtain the search direction and step length. Both the *active set* algorithm and the *SQP* algorithm use Sequential Quadratic Programming as a minimization strategy. Here, Newton's method is mimicked by approximating the Hessian of the Lagrangian function using a quasi-Newton updating method. The *active set* algorithm in addition uses an estimate of which constraints are active at each iteration to reduce the complexity of the problem.

## B. Bounds

When setting bounds on variables, you would like to restrain your design space as little as possible, in order to capture all possible design combinations. However, restraining the design space simplifies the optimization procedure and can reduce time consumption. What is particularly important is to not allow for "unphysical" behavior of the model. Take as an example the slot width. If the lower bound on slot width is 0, then for the lowest allowable values, the winding width will actually become negative. This leads to negative current and negative torque, negative active length and negative cost. Of course it is possible to set constraints keeping winding width and winding height positive, but once the solver moves in this area of the design space, it can be difficult to find the direction towards the feasible area, and the optimization fails to find a feasible solution. To avoid this problem, the lower bounds on slot depth and slot width are set according to main wall insulation thickness and slot wedge thickness.

The variable's bounds are listed in Table II. The upper bound on the outer diameter is chosen because a machine with a bigger diameter must be split into sections, both for production convenience and transportation limitations. A bigger diameter would increase the cost of production and assembly.

The intention of the upper bound on current density is to prevent overheating, and the value is based on recommendations given in [20]. For further improvement of the model, a thermal calculation can be added, and constraints put on machine temperatures. The lower bound on stator and rotor yoke thickness and magnet thickness will ensure a certain mechanical stability.

## C. Constraints

Constraints are set on various parameters in order to prevent a machine design that cannot be made in practice, or that will lead to unnecessary costs in other parts of the tidal energy system. The upper limit on frequency is set to keep converter costs down. A constraint is put on tooth width for mechanical strength, and on active length for both transportation reasons and thermal expansion. The power factor is constrained to be above 0.85 based on expectations from the tidal energy industry. Another constraint to ensure sufficient cooling is put on current loading. Finally, magnetic flux density in stator and rotor yoke and stator teeth are kept low enough to prevent saturation.

## D. Objective function

Two different objective functions are investigated; weight of active materials and cost of active materials,  $f(X)$  (both including housing):

$$f(X) = M_{s,y}C_{lam} + M_{cond}C_{cond} + (M_{r,y} + M_{house})C_{steel} + M_{pm}C_{pm} \quad (5)$$

where  $M_{s,y}, M_{cond}, M_{r,y}, M_{house}$  and  $M_{pm}$  are weights of stator yoke, conductors, rotor yoke, housing and permanent magnets, respectively, and  $C_{lam}, C_{cond}, C_{steel}$  and  $C_{pm}$  are

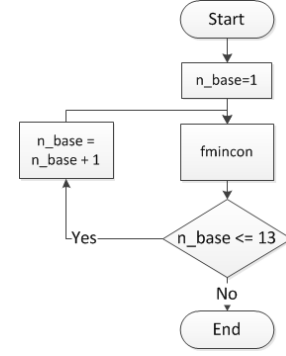


Fig. 4. Flowchart of integer number grid search

cost per kilogram of laminations, conductors, steel and permanent magnets. Costs are set based on former experience, and are not exact, as they will vary with dimensions, machining, supplier et cetera. However, the cost parameters include, as far as possible, the costs related to production. For magnets, coating and machining is included, for laminations, stamping and stacking is included, and for winding wires, insulation is included.

## E. Integer variables

As explained, the gradient based solver is unable to use integer variables as input. Because the number of base windings must be an integer number, and there are only a limited number of possibilities due to the limitation in electrical frequency, a basic grid-search is performed, investigating the optimum at each possible base winding number. The procedure is illustrated in Figure 4. The variable  $n_{base}$  maximum is set to 13, because of the frequency constraint.

TABLE III  
CONSTRAINTS

Parameter	
Efficiency	$\geq 0.96$
Power factor	$\geq 0.85$
Current loading	$\leq 35$ kA/m
Frequency	$\leq 200$ Hz
Tooth width	$\geq 5$ mm
Distance between magnets	$\geq 1$ mm
$w_{wind}$	$\geq 1$ mm
$h_{wind}$	$\geq 1$ mm
Mechanical stress	$\leq 30$ MPa
Inner diameter	$\geq 0$ m
Tooth flux density	$\leq 1.5$ T
Stator yoke flux density	$\leq 1.1$ T
Rotor yoke flux density	$\leq 0.9$ T
Length	$\leq 4$ m

TABLE IV  
FMINCON ALGORITHMS

Algorithm	Objective value	Solution time	Iterations
interior point	92 547 EUR	111 s	71
sqp	91 672 EUR	122 s	65
active set	91 947 EUR	105 s	69

## IV. RESULTS

### A. Appropriate algorithm

Firstly, the different algorithms available for using the *fmincon* solver in MATLAB are investigated, trying to establish which is best suited for this problem. The *trust region reflective* algorithm cannot be used in problems with nonlinear constraints, and therefore cannot be used. Recommendations given by the software states that the *interior point* algorithm should be used first, and to obtain more speed, the *sqp* can be tried, and thereafter *active set*. The problem was run for all three algorithms with  $n_{base}$  set to 7 and the bounds shown in Table II, and only the *interior point* algorithm was able to present a result. By investigating the bounds settings, it was clear that the lower bound on current density set to zero was the cause of the malfunction. By increasing this to a positive value, all algorithms provided approximately the same optimal result. Table IV shows the resulting objective value, solution time and number of iterations used for each algorithm. All algorithms have comparable solution times, and the *sqp* algorithm finds the best solution, 0.9 % lower than the *interior point* result. When searching for multiple minimas using *MultiStart*, described further below, the *active set* algorithm could not provide a result. Based on these findings, both the *interior point* and the *sqp* algorithm can be recommended for electrical machine design optimization.

### B. Two different objective functions

Going forward with the chosen algorithm, two optimization processes are performed, with two different objective functions; weight and cost. The results are listed in Table V. The machines are similar, both in size, shape and cost. The cost optimized machine is only 0.5 % cheaper and 0.9 % heavier than the weight optimized machine. A reason for the small difference is the very tight constraint on efficiency, which gives a narrow design space of feasible solutions.

The solution is constrained by the following parameters: Maximum outer diameter, minimum power factor, minimum efficiency and maximum flux density in the rotor yoke. The solution will improve if either of these constraints are relaxed, and deteriorate or become infeasible if they are restricted.

Table VI shows a similar case, but with the constraint on efficiency removed. For this, less constrained model, the difference between the two objective functions becomes clear. The cost optimized machine is 31 % cheaper and 21 % heavier than the weight optimized machine. Note especially the difference in PM weight, which has by far the highest cost per kilogram. In many cases of machine optimization, weight is minimized, while cost is the real target. A reason why weight is chosen is that the price of materials is not easily accessible, and depends on many factors, but even a good guess may result in a better design, if low cost is your true target.

### C. Global minimum

As the gradient based optimization is not capable of finding the global minimum, a search is done to investigate the pres-

TABLE V  
OPTIMIZED MACHINE PARAMETERS

	Weight optimized machine	Cost optimized machine
Cost	92 121 EUR	91 782 EUR
Weight	11 353 kg	11 370 kg
Variables		
$D_{outer}$	3.5 m	3.5 m
$d_{s,yoke}$	26 mm	26 mm
$d_{slot}$	59 mm	58 mm
$w_{slot}$	20 mm	19 mm
$l_m$	6 mm	6 mm
$\alpha_m$	0.965	0.962
$d_{r,yoke}$	32 mm	32 mm
$J$	3.22 A/mm <sup>2</sup>	3.38 A/mm <sup>2</sup>
$n_{base}$	7	7
Machine parameters		
Length	815 mm	819 mm
Efficiency	96 %	96 %
Power factor	0.85	0.85
Current loading	26 315 A/m	26 083 A/m
Copper weight	743 kg	705 kg
Magnet weight	362 kg	359 kg
Iron weight	6 433 kg	6 470 kg

TABLE VI  
OPTIMAL LOW EFFICIENCY MACHINE

	Cost optimized machine	Weight optimized machine
Cost	97 011 EUR	66 578 EUR
Weight	5 461 kg	6 615 kg
Variables		
$D_{outer}$	3.5 m	3.5 m
$d_{s,yoke}$	11 mm	12 mm
$d_{slot}$	37 mm	51 mm
$w_{slot}$	22 mm	17 mm
$l_m$	24 mm	8 mm
$\alpha_m$	0.886	0.914
$d_{r,yoke}$	20 mm	15 mm
$J$	4 A/mm <sup>2</sup>	4 A/mm <sup>2</sup>
$n_{base}$	11	11
Machine parameters		
Length	478 mm	613 mm
Efficiency	91.8 %	94.6 %
Power factor	0.97	0.85
Current loading	35 000 A/m	35 000 A/m
Copper weight	479 kg	591 kg
Magnet weight	809 kg	353 kg
Iron weight	1 884 kg	2 805 kg

ence of other minimas within the feasible region. A *MultiStart* run with  $n_{base}$  fixed at 7, starting the search from 10 different initial points was performed. Unless all startpoints are manually specified, *MultiStart* randomly chooses starting points based on the variable bounds. For unbounded variables the starting point values become very high, and the minimization algorithm is unable to find a solution. The following variables are given new bounds;  $d_{s,yoke}$  Upper Bound (UB) 30 cm,  $d_{slot}$  UB 30 cm,  $w_{slot}$  UB 50 cm,  $\alpha_m$  Lower Bound (LB) 0.5,  $d_{r,yoke}$  UB 30 cm. No results were obtained with the *active set* algorithm. The *interior point* algorithm found two minimas, while the *sqp* algorithm found 6 minimas, the best one very similar to the machine geometry presented in Table V, column

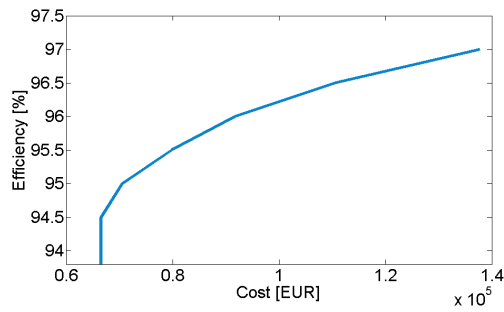


Fig. 5. Efficiency versus cost

3. The best cost found was 91 656 EUR. The five best solutions have similar geometries, and costs varying by 6 %. The last minimum has a cost 3.7 times the best cost. This shows that several minimas exist within the feasible region, and that the choice of starting point is of crucial importance.

Another try was made to find alternative minimas, with the use of a GA optimization, also done in Matlab. With the bounds presented in Table II, the solver was unable to even find a feasible solution. By setting the same bounds as for the *MultiStart* the GA found a machine design with a cost of 93 226 EUR, and variables in close range of the gradient based optimized machine. The solution time is considerably longer. With the global searches performed here, it is assumed that the found solution is, indeed, the global minimum, although it is in theory possible that a better minimum exists.

#### D. Efficiency constraint

It is of interest to investigate the effect on cost that the constraint on efficiency has. A new optimization process is performed, and the result is shown in Table VI. With the given constraints, the cost optimal machine has an efficiency of 94.6 % and the cost is down by 27 %. The dramatic decrease of cost should make the designer consider reducing the efficiency of the machine. This must be weighed against the cost of lost energy production for the tidal turbine. The pareto curve drawn in Figure 5 further illustrates this interaction, showing efficiency as a function of cost.

In this case, the active constraints are on power factor, current loading, current density, flux density in stator and rotor yoke and maximum outer diameter. With the thermal constraints on both current density and current loading active, there is a risk of high temperatures in the machine. A thermal model should be made to check the feasibility of the design.

#### E. Other constraints

A sensitivity analysis is of interest for the machine designer, and can help setting sensible constraints. The active constraints in the optimal point, in addition to efficiency, are maximum outer diameter, minimum power factor and maximum flux density in the rotor yoke. An increase in outer diameter will result in a segmented design, where machine structures are manufactured in several pieces and assembled on site. This is costly, but it can be worth investigating the potential savings in material cost. Removing the upper bound on outer diameter

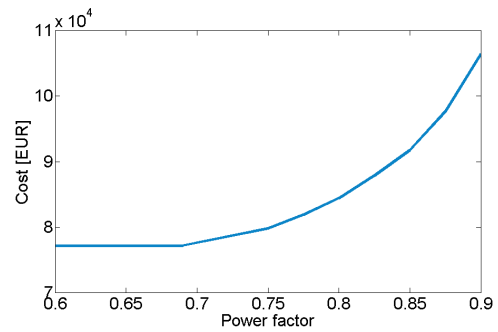


Fig. 6. Cost versus power factor

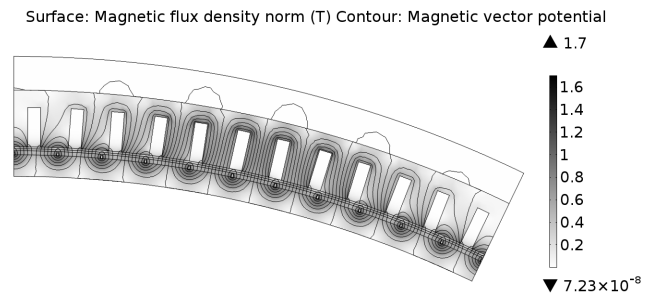


Fig. 7. Flux density distribution in machine

results in an optimal design, when optimizing for cost, with a material cost of 66 292 EUR, 72 % of the original cost, and an outer diameter of 8.59 m. In the case of tidal turbines, the hydrodynamics of the turbine will not allow for such a big diameter, so this is not a practical solution in this particular case.

The power factor of the machine decides the MVA rating of the electrical system, and therefore the cost of other parts, like the power converter. It is desirable to keep it as high as possible, but this leads to higher machine cost. An optimum exists for the total system, and to find this it is of interest to see the correlation. Figure 6 illustrates how machine cost varies with the constraint on power factor. The minimum cost is achieved when the power factor is 0.69.

#### F. FEA verification

A FEA model is built to verify the analytical calculations. The geometry presented in table V, column 3, is used, and the resulting magnetic flux density field is shown in figure 7. Calculated performance using the analytical tool and the FEA tool are listed in VII. The results show a satisfactory match between analytical results and FEA results. The biggest difference is in the inductance calculation, implying that the real power factor will likely be somewhat lower than the analytically calculated one. A revision of the inductance calculation would improve the model. It is worth noting that the total harmonic distortion of the induced voltage is approximately 9 %, which is fairly high. A smaller ratio of magnet width to pole pitch would reduce this.

TABLE VII  
COMPARISON OF ANALYTICAL AND FEA RESULTS

Parameter	Analytical	FEA	ratio
Induced voltage, 1. harm.	1 755 V	1 729 V	0.986
Electromagnetic torque	179.05 kNm	171.99 kNm	0.961
No-load tooth flux	24.0 mWb	26.3mWb	1.096
Phase inductance	5.70 mH	6.72 mH	1.18
No-load iron loss	12 990 W	13 421 W	1.033

## V. CONCLUSION

It is shown that gradient based optimization techniques can be applied to PM machine design, but the starting point is important to find the global minimum. An optimal generator for a tidal turbine with a central shaft and a one stage gear is presented. When using solvers available from the MATLAB library, it can be recommended to choose the *interior point* or the *sqp* algorithm within the *fmincon* solver for robust and fast optimization. While gradient based solvers are only able to find local minimas, one can search for multiple minimas using the *MultiStart* function, or even a GA. A major drawback of gradient based search strategies is the inability to use integer variables. For few integer variables, say one or two, and narrow variable space, it is possible to create a basic grid search to account for this. For a higher number of integer variables, it is recommended to use a stochastic method.

The solver was able to find a feasible solution with a high efficiency within a very small feasible area. A genetic algorithm search with the same bounds was unable to find this, and bounds had to be narrowed down, even with one variable fixed, in order to find a solution. The choice of objective value is very important for the optimization model, although, in this case, with the small region of feasibility, a machine optimized for cost and weight gave very similar results.

The effect of changing bounds and constraints was illustrated, and curves were drawn to show how efficiency and power factor constraints affect machine cost. It is illustrated how the optimization tool can be used by the designer to make good choices for the design of the whole system.

Further improvement of the work could include a thermal model, where constraints are put on magnet and winding temperature instead of current density and current loading. A development of the cost function could include the cost of energy loss, cost of the power converter and cost of the mechanical structure.

## ACKNOWLEDGMENT

The author would like to thank SmartMotor AS for funding and for sharing knowledge about trends in the tidal market and help with analytical models.

## REFERENCES

- [1] A. Røkke and R. Nilssen, "Marine current turbines and generator preference. a technology review," *Renewable Energy and Power Quality Journal*, vol. 11, no. 299, March 2013.
- [2] N. Bianchi and S. Bolognani, "Design optimisation of electric motors by genetic algorithms," *IEE Proceedings-Electric Power Applications*, vol. 145, no. 5, pp. 475–483, 1998.

- [3] F. Cupertino, G. Pellegrino, E. Armando, and C. Gerada, "A syr and ipm machine design methodology assisted by optimization algorithms," in *2012 IEEE Energy Conversion Congress and Exposition (ECCE)*, 2012, pp. 3686–3691.
- [4] J. Vasconcelos, R. Saldanha, L. Krähenbühl, and A. Nicolas, "Genetic algorithm coupled with a deterministic method for optimization in electromagnetics," *IEEE Transactions on Magnetics*, vol. 33, pp. 1860–1863, 1997.
- [5] Y. Duan and D. M. Ionel, "A review of recent developments in electrical machine design optimization methods with a permanent magnet synchronous motor benchmark study," in *Energy Conversion Congress and Exposition (ECCE)*. IEEE, 2011, pp. 3694–3701.
- [6] H. Li, Z. Chen, and H. Polinder, "Optimization of multibrid permanent-magnet wind generator systems," *IEEE Transactions on Energy Conversion*, vol. 24, no. 1, pp. 82–92, 2009.
- [7] T. Hamiti, C. Gerada, and M. Rottach, "Weight optimisation of a surface mount permanent magnet synchronous motor using genetic algorithms and a combined electromagnetic-thermal co-simulation environment," in *Energy Conversion Congress and Exposition (ECCE), 2011 IEEE*, 2011, pp. 1536–1540.
- [8] J.-S. Chun, H.-K. Jung, and S.-Y. Hahn, "A study on comparison of optimization performances between immune algorithm and other heuristic algorithms," *IEEE Transactions on Magnetics*, vol. 34, no. 5, pp. 2968–2971, 1998.
- [9] M. Farina and J. Sykulski, "Comparative study of evolution strategies combined with approximation techniques for practical electromagnetic optimization problems," *IEEE Transactions on Magnetics*, vol. 37, no. 5, pp. 3216–3220, 2001.
- [10] M. Van der Geest, H. Polinder, J. A. Ferreira, and D. Zeilstra, "Optimization and comparison of electrical machines using particle swarm optimization," in *Electrical Machines (ICEM), 2012 XXth International Conference on*, Sept 2012, pp. 1380–1386.
- [11] Y. Ahn, J. Park, C.-G. Lee, J.-W. Kim, and S.-Y. Jung, "Novel memetic algorithm implemented with ga (genetic algorithm) and mads (mesh adaptive direct search) for optimal design of electromagnetic system," *IEEE Transactions on Magnetics*, vol. 46, no. 6, pp. 1982–1985, 2010.
- [12] O. Mohammed and G. Üler, "A hybrid technique for the optimal design of electromagnetic devices using direct search and genetic algorithms," *IEEE Transactions on Magnetics*, vol. 33, no. 2, pp. 1931–1934, 1997.
- [13] T. Raminosa, I. Rasoanarivo, F.-M. Sargos, and R. Andriamalala, "Constrained optimization of high power synchronous reluctance motor using non linear reluctance network modeling," in *41st IAS Annual Meeting (IEEE Industry Applications Society)*, 2006, pp. 1201–1208.
- [14] J. Legranger, G. Friedrich, S. Vivier, and J. Mipo, "Combination of finite-element and analytical models in the optimal multidomain design of machines: Application to an interior permanent-magnet starter generator," *IEEE Transactions on Industry Applications*, vol. 46, no. 1, pp. 232–239, 2010.
- [15] D. C. Hanselman, *Brushless permanent-magnet motor design*. McGraw-Hill New York, 1994.
- [16] C. Mi, G. Slemmon, and R. Bonert, "Modeling of iron losses of surface-mounted permanent magnet synchronous motors," in *Industry Applications Conference, 2001. Thirty-Sixth IAS Annual Meeting. Conference Record of the 2001 IEEE*, vol. 4, Sept 2001, pp. 2585–2591 vol.4.
- [17] M. Shah and S. Lee, "Rapid analytical optimization of eddy-current shield thickness for associated loss minimization in electrical machines," *IEEE Transactions on Industry Applications*, no. 3, pp. 642–649, 2006.
- [18] E. Fornasiero, "Advanced design of direct drive pm machines," 2010.
- [19] MathWorks. (2013, June) Constrained nonlinear optimization algorithms. MathWorks. [Online]. Available: <http://www.mathworks.se/help/optim/ug/constrained-nonlinear-optimization-algorithms.html>
- [20] J. Pyrhonen, T. Jokinen, and V. Hrabovcová, *Design of rotating electrical machines*. Wiley, 2009.

**Astrid Røkke** received the MSc degree in electrical engineering from the Norwegian University of Science and Technology (NTNU) in 2007. From 2007 to 2012 she was employed by SmartMotor AS working with development of permanent magnet machines. Currently she is a PhD student at the department of electric power engineering at NTNU. Her special fields of interest include modeling and simulation of electrical machines.